

Electronic Supplementary Information

Graphene oxide/graphene vertical heterostructure electrodes for high efficient and flexible organic light emitting diodes

S. Jia,^a H. D. Sun,^b J. H. Du,^{a} Z. K. Zhang,^a D. D. Zhang,^a L. P. Ma,^a J. S. Chen,^b D. G.*

Ma,^{b} H. M. Cheng,^a and W. C. Ren^{a*}*

^a Shenyang National Laboratory for Materials Science, Institute of Metal Research, Chinese Academy of Sciences, 72 Wenhua Road, Shenyang 110016, P. R. China, E-mail: jhdu@imr.ac.cn; wren@imr.ac.cn.

^b State Key Laboratory of Polymers Physics and Chemistry, Changchun Institute of Applied Chemistry, Chinese Academy of Sciences, 5625 Renmin Street, Changchun 130022, P. R. China, E-mail: mdg1014@ciac.ac.cn.

1. XPS characterization of monolayer graphene after ozone treatment for different time

XPS was used to characterize the structure change of monolayer graphene after ozone treatment for different time. As shown in **Figure S1**, no evident peaks were found around 286 and 288 eV except for the C-C peak at ~284.6 eV, indicating no oxygen functional groups in pristine graphene. With extending ozone treatment time, the oxygen functional groups-related peaks around 286 and 288 eV appear and begin to grow up, indicating gradual oxidation of graphene. The ratio of the peak areas of oxygen-bonded carbon to sp² carbon (G-O/G) increases sharply from 10.8% to 16.0% when the ozone treatment time is increased from 5 min to 10 min. However, a further increase to 15 min only results in a small increase to 17.2%.

These results indicate that the oxidation of monolayer graphene becomes almost saturated after 10 min ozone treatment, which is consistent with the optical transmittance change (Figure 2b in the main text).

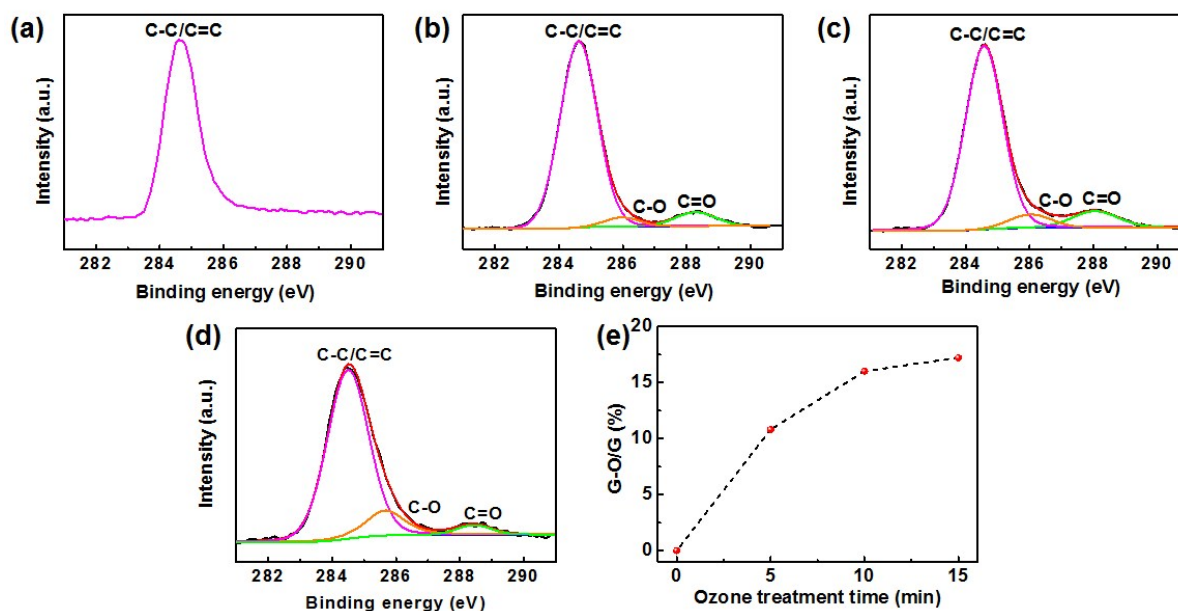


Figure S1. (a)-(d) C1s XPS spectra of a monolayer graphene film after ozone treatment for (a) 0 min, (b) 5 min, (c) 10 min, (d) 15 min. (e) Peak area ratio of G-O/G estimated from the areas of C-O, C=O and C-C/C=C peaks as a function of ozone treatment time.

2. Raman spectra of monolayer graphene and three-layer graphene films with different ozone treatment time

As shown in Figure S2a, the CVD grown graphene shows a G band around 1580 cm^{-1} and a very strong symmetrical 2D band at 2680 cm^{-1} . The very small D band indicates the presence of disorders, defects and grain boundaries, which are frequently observed in CVD grown graphene. After 5 min ozone treatment, the intensity of the disorder-related D band increases dramatically along with the appearance of a G' band. The presence of a small upshifted 2D band indicates that the monolayer graphene is not fully oxidized but heavily hole-doped. However, after 10 min ozone treatment, the monolayer graphene shows a similar Raman characteristic to fully oxidized graphene oxide, which shows almost no change even after

extending the ozone treatment time to 15 min. These results indicate that the oxidation of the monolayer graphene film become almost saturated after 10 min ozone treatment, which is consistent with XPS, optical transmittance and sheet resistance measurements.

As shown in **Figure S2b**, P-TLG shows similar Raman features to pristine monolayer graphene film but the intensities of the G and 2D bands are almost 3 times stronger than those of pristine monolayer graphene because the neighbouring layers in P-TLG are decoupled. As shown in Figure S2a, the 2D band is almost completely suppressed when oxidation becomes saturated after 10 min ozone treatment for monolayer graphene. Moreover, it is well known that hole-doping of graphene can lead to an extraction of the crystal lattice, and consequently, a stiffening of phonons and an upshift of the 2D band along with a dramatic decrease in its intensity.¹⁻³ Therefore, the small decrease in the I_{2D}/I_G intensity ratio from 1.3 to 0.98 (the decrease is smaller than 1/3) and the upshift of the 2D band after 5 min ozone treatment indicate that the top layer of the three-layer graphene is not fully oxidized but hole-doped. In contrast, the 2D band upshifts dramatically by $\sim 8\text{ cm}^{-1}$ and the I_{2D}/I_G intensity ratio decreases significantly from 1.3 to 0.68 (the decrease is more than 1/3) when the top layer is fully oxidized after 10 min ozone treatment. Considering that the 2D band almost completely disappeared for monolayer graphene when it was fully oxidized after 10 min ozone treatment, the upshifted 2D peak of S-GO/G originates from the two underneath layers, giving strong evidence that the underneath graphene layers are p-doped by top layer GO. Note that the G peak also upshifts from $\sim 1582\text{ cm}^{-1}$ to 1587 cm^{-1} because of the stiffening of phonons induced by hole doping, which is consistent with the 2D peak shift. Similar to GO, in the ozone-treated graphene, the oxygen bonded with carbon atoms distorts graphene plane in some areas and consequently might generate some strain. However, for TLG films obtained by layer-by-layer transfer, even strain might be generated on the top layer, it is hard to affect the underlying graphene films due to the weak interlayer coupling. The very strong D peak of S-GO/G indicates the presence of lots of disorders in the oxidized top layer. Extending the

ozone treatment time to 15 min leads to a further decrease in I_{2D}/I_G intensity ratio and a small upshift of the 2D band, indicating that the underlying graphene layer was also oxidized because ozone molecules can penetrate into the underlying graphene through grain boundaries and defects in the top layer. This is consistent with the results deduced from the transmittance change shown in the main text.

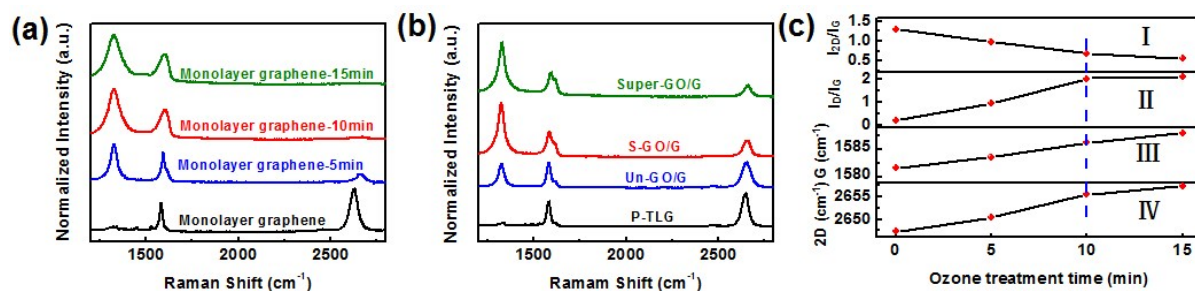


Figure S2. G-peak intensity normalized Raman spectra of (a) a monolayer graphene and (b) a three-layer graphene film with different ozone treatment time. (c) (I) I_{2D}/I_G intensity ratio, (II) I_D/I_G intensity ratio, (III and IV) position changes of (III) G band and (IV) 2D band of a three-layer graphene film as a function of ozone treatment time.

3. Sheet resistance and transmittance of graphene films with different numbers of layers and different ozone treatment time

As shown in **Figure S3a-b**, the sheet resistances of monolayer, two-layer, and three-layer pristine graphene films are 867, 446, and 263 ohm sq⁻¹, respectively, and the corresponding transmittances at 550 nm wavelength are 97.0, 94.1, and 90.7%. The presence of small islands on the surface of monolayer graphene films leads to the small transmittance difference from that of perfect monolayer graphene (97.7%). The transmittance of three-layer graphene and monolayer graphene films increases with ozone treatment time, as shown in **Figure S3c-d**. It is well established that the oxidation could change graphene from sp² hybridization to sp³ hybridization and consequently destroy the electronic conjugation of graphene and decrease its absorption. Therefore, the continuous increase in transmittance with ozone treatment time is

attributed to the continuous decrease of sp^2 fraction in ozone-treated graphene as confirmed by XPS data shown in **Figure S1**.

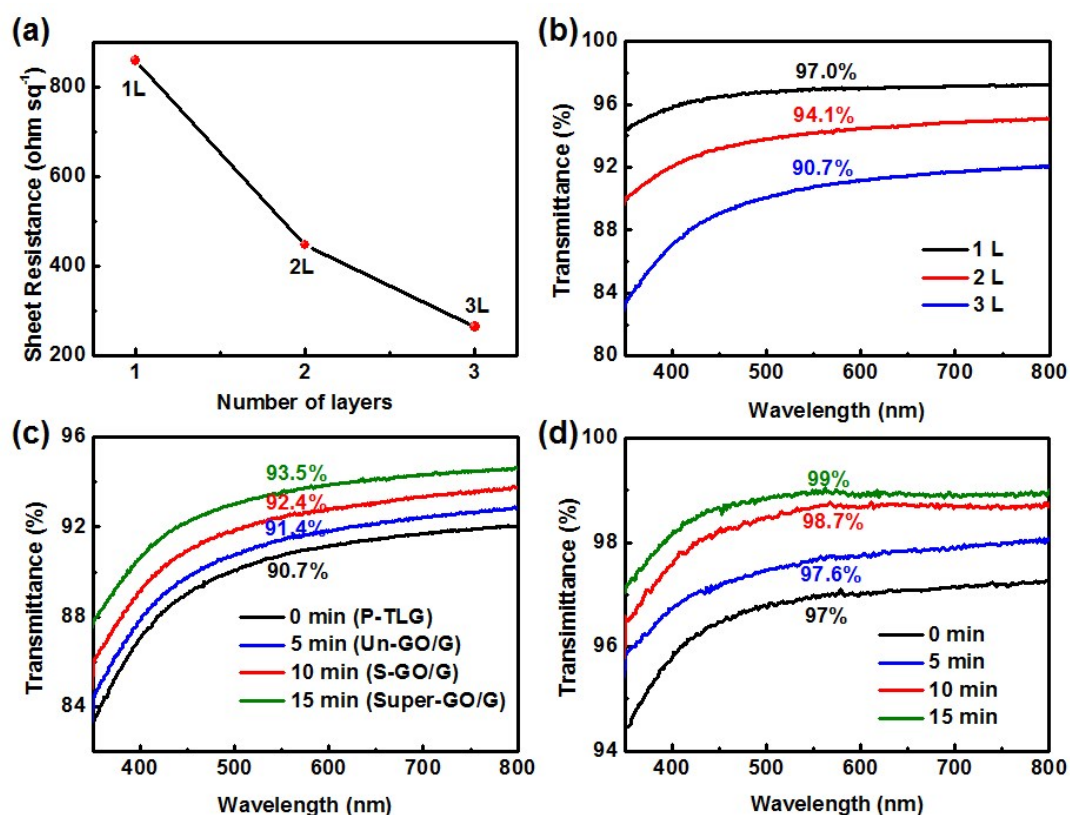


Figure S3. (a) Sheet resistance and (b) transmittance of pristine graphene films with different numbers of layers. Transmittance of (c) a three-layer graphene and (d) a monolayer graphene film with different ozone treatment time.

4. Doping effect of MoO₃ on graphene and GO/G electrodes

It has been reported that thermally evaporated MoO₃ could dope graphene to reduce its sheet resistance by charge transfer.^{4, 5} We also checked the sheet resistances of P-TLG and GO/G electrodes after MoO₃ doping (**Figure S4**) and found that they can be decreased by 24% and 11% in inert atmosphere, respectively. This doping effect should have a positive influence on the performance of OLEDs with graphene anodes. However, the changes of sheet resistances could not be detected under ambient conditions. This is probably attributed to the weak stability of doping effect of MoO₃ under ambient conditions,^{6, 7} which is dramatically

different from the stable doping effect of GO.

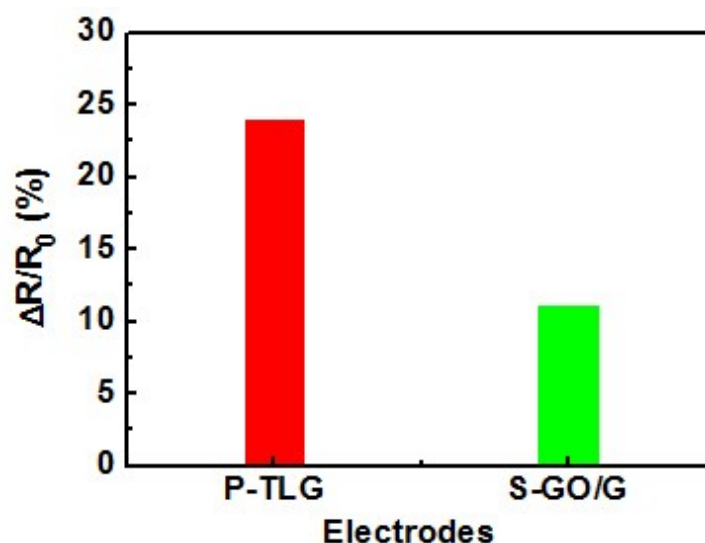


Figure S4. Sheet resistance decrease of P-TLG and S-GO/G electrodes after MoO₃ doping.

5. Performance of green OLEDs with different anodes

Figure S5 shows the current density and luminance vs voltage characteristics of green OLEDs with ITO, P-TLG and GO/G heterostructure anodes. It is found that the current densities of OLEDs with graphene-based anodes are lower than that of device with an ITO anode at the same driving voltage. This is because the sheet resistance of graphene-based anodes ($>200 \text{ ohm sq}^{-1}$ for the S-GO/G heterostructure) is significantly larger than that of ITO ($\sim 10 \text{ ohm sq}^{-1}$). However, the luminance difference is very small for the OLEDs with graphene-based and ITO anodes. For example, the OLEDs with S-GO/G heterostructure anodes show almost the same luminance with those with an ITO anode at a driving voltage of 3.0 V. This is because that the device resistance adds up from all series resistance in the device, that is, from bulk transport, interface transfer, transport through the contacts and resistance of electrodes, *etc.* Since the active area of our devices is small (about $4 \times 4 \text{ mm}^2$), the effect of electrode resistance is significantly reduced. While the higher work function and better compatibility with MoO₃ of S-GO/G anode may cause a much smaller barrier and interface resistance for hole injection and transportation. As a result, the relatively larger voltage drop

of OLED with S-GO/G anode caused by electrode resistance could be partially or entirely compensated by the smaller voltage drop caused by the smaller energy barrier and interface resistance at GO/G and MoO₃ interface.

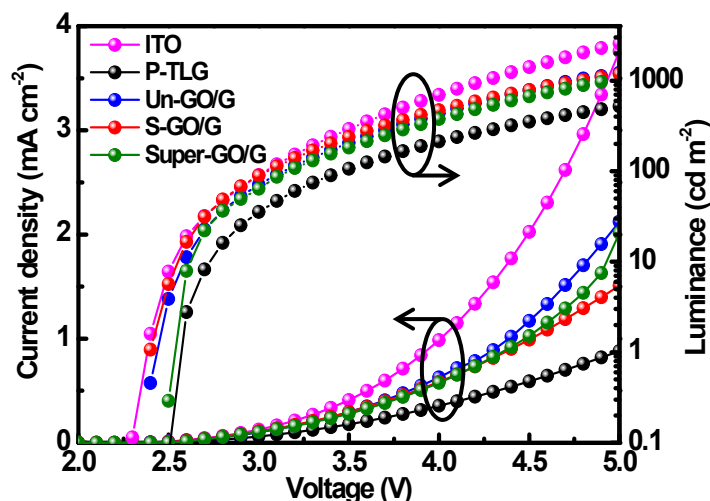


Figure S5. Current density and luminance vs voltage characteristics of green OLEDs with ITO, P-TLG and GO/G heterostructure anodes.

Table S1 list the performances and device structures of green OLEDs with graphene anodes in the literature. It can be found that the efficiency of almost all OLEDs with graphene anodes is less than 10 lm W⁻¹, much lower than that with ITO anodes and far from satisfactory. Han et al. achieved a very high PE (about 102.7 lm W⁻¹) with HNO₃ doped graphene as anodes. However, this TCE might seriously influence the stability of OLEDs since the sheet resistance of graphene TCEs doped with HNO₃ increased about 30% in only one day under ambient conditions. In this work, we used S-GO/G heterostructures as anodes to achieve a very high PE of 98.2 lm W⁻¹, which is 10 times more than most previous work and comparable to that based on HNO₃ doped graphene as anodes. More importantly, our device is expected to have a much better stability since the doping effect of the S-GO/G

heterostructure remains stable for several months under ambient conditions (**Figure 2d-e**), showing great potential for practical applications.

Table S1. Comparison of the device structures and performances of green OLEDs with different graphene-based anodes

Reference	Graphene TCEs	Device structure	Maximum CE (cd A ⁻¹)	Maximum PE (lm W ⁻¹)
33	Multilayer (about 20)	G/V ₂ O ₅ /NPB/CBP:Ir(ppy) ₂ (acac)/Bphen/Bphen:Cs ₂ CO ₃ /Sm/Au	0.75	0.38
34	Monolayer	G/MoO ₃ /NPB:MoO ₃ /TAPC/CBP:Ir(ppy) ₂ (acac)/TPBi/Liq/Al	11.44	2.24
35	Monolayer	G/TiO _x /PEDOT:PSS/NPB/Alq ₃ :C545T/Alq ₃ /LiF/Al	10.11	10.0
36	Bilayer	G/V ₂ O ₅ /NPB/Alq ₃ /Bphen:Cs ₂ CO ₃ /Sm/Au	1.18	0.41
37	Reduced GO and PEDOT:PSS composite (rGC)	rGC/PEDOT:PSS/TPD/Alq ₃ /LiF/Al	3.9	1.22
30	Reduced GO (rGO)	rGO/PEDOT:PSS/NPD/Alq ₃ /LiF/Al	0.2	0.35
27	Multilayer (4 layer)	G/GraHIL/NPB/Bebq ₂ :C545T/Bebq ₂ /Liq/Al	30.2	37.2
		G/GraHIL/TAPC/TCTA:Ir(ppy) ₃ /CBP:Ir(ppy) ₃ /TPB/LiF/Al	98.1	102.7
Our work	GO/G heterostructure	G/GO/MoO ₃ /TAPC/Ir(ppy) ₂ (acac):TCTA/Ir(ppy) ₂ (acac):Bphen/Bphen/Li/Al	82.0	98.2

6. Introduction to the movie

The movie shows OLEDs with S-GO/G heterostructure anodes before and during operation. Before operating, we first repeatedly bent the devices, and found that the OLEDs still can be

normally illuminated after bending many times. More importantly, during the light emission process, repeated bending also has no significant influence on the luminance characteristics of the device, indicating the excellent flexibility of the GO/G heterostructure TCEs and the corresponding OLED devices.

References

- 1 A. Das, S. Pisana, B. Chakraborty, S. Piscanec, S. Saha, U. Waghmare, K. S. Novoselov, H. R. Krishnamurthy, A. K. Geim, A. C. Ferrari and A. K. SOOD, *Nat. Nanotechnol.*, 2008, **3**, 210.
- 2 L. Pietronero and S. Strassler, *Phys. Rev. Lett.*, 1981, **47**, 593.
- 3 J. E. Lee, G. Ahn, J. Shim, Y. S. Lee and S. Ryu, *Nat. Commun.*, 2012, **3**, 1024
- 4 S. L. Hellstrom, M. Vosgueritchian, R. M. Stoltenberg, I. Irfan, M. Hammock, Y. B. Wang, C. Jia, X. F. Guo, Y. L. Gao and Z. Bao, *Nano Lett.*, 2012, **12**, 3574.
- 5 J. Meyer, P. R. Kidambi, C. B. Bernhard, C. Weijtens, A. Kuhn, A. Centeno, A. Pesquera, A. Zurutuza, J. Robertson and S. Hofmann, *Sci. Rep.*, 2014, **4**, 5380.
- 6 Irfan, H. Ding, Y. Gao, C. Small, D. Y. Kim, J. Subbiah and F. So, *Appl. Phys. Lett.*, 2010, **96**, 243307.
- 7 L. F. Xie, X. Wang, H. Y. Mao, R. Wang, M. Z. Ding, Y. Wang, B. Özyilmaz, K. P. Loh, A. T. S. Wee, Ariando and W.Chen, *Appl. Phys. Lett.*, 2011, **99**, 012112.